

# Nuclear fusion catalyzed by doubly charged scalars: Implications for energy production

Evgeny Akhmedov<sup>✉\*</sup>*Max-Planck-Institut für Kernphysik, Saupfercheckweg 1, 69117 Heidelberg, Germany* (Received 13 October 2021; accepted 15 July 2022; published 12 August 2022)

A number of popular extensions of the Standard Model of particle physics predict the existence of doubly charged scalar particles  $X^{\pm\pm}$ . Such particles may be long lived or even stable. If they exist,  $X^{--}$  could form atomic bound states with light nuclei and catalyze their fusion by essentially eliminating the Coulomb barrier between them. Such an  $X$ -catalyzed fusion (XCF) process does not require high temperatures or pressure and may have important applications for energy production. A similar process of muon-catalyzed fusion has been shown not to be a viable source of energy because of the sticking of negative muons to helium nuclei produced in the fusion of hydrogen isotopes, which stops the catalytic process. We analyze XCF in deuterium environments and show that the  $X$  particles can only stick to  ${}^6\text{Li}$  nuclei, which are produced in the third-stage reactions downstream in the catalytic cycle. The corresponding sticking probability is very low and, before getting bound to  ${}^6\text{Li}$ , each  $X$  particle can catalyze  $\sim 3.5 \times 10^9$  fusion cycles, producing  $\sim 7 \times 10^4$  TeV of energy. We also discuss the ways of reactivating the  $X$  particles from the Coulomb-bound ( ${}^6\text{Li}X$ ) states, which would allow reusing them in XCF reactions.

DOI: [10.1103/PhysRevD.106.035013](https://doi.org/10.1103/PhysRevD.106.035013)

## I. INTRODUCTION

A number of popular extensions of the Standard Model (SM) of particle physics predict the existence of doubly charged scalar particles  $X^{\pm\pm}$ . These include the type-II seesaw [1–6] and the Zee-Babu [7,8] models of neutrino masses, the left-right model [9–11], the Georgi-Machacek model [12–16], the 3-3-1 model [17,18] and the little Higgs model [19]. Doubly charged scalars appear also in simplified models, in which one merely adds such scalars in a gauge-invariant way in various representations of the SM gauge group  $SU(2)_L$  to the particle content of the SM. The Lagrangian of the model is then complemented by gauge-invariant interaction terms involving these new fields [20,21].

Doubly charged scalars may be long lived or even stable [21–24]. As the simplest example, one can add to the SM an uncolored  $SU(2)_L$ -singlet scalar field  $X$  with hypercharge  $Y = 2$  [21]. The corresponding doubly charged particles will couple to the neutral gauge bosons  $\gamma$  and  $Z^0$  and may also interact with the SM Higgs boson  $H$  through

the  $(H^\dagger H)(X^\dagger X)$  term in the Higgs potential. Gauge invariance allows, in addition, the Yukawa coupling of  $X$  to right-handed charged leptons,  $h_X l_R l_R X + \text{H.c.}$  This is the only coupling that makes the  $X$  particles unstable in this model; they will be long lived if the Yukawa coupling constants  $h_X$  are small. The Yukawa coupling of  $X$  may be forbidden by, e.g.,  $Z_2$  symmetry  $X \rightarrow -X$ , in which case the  $X$  scalars will be stable.

Doubly charged scalar particles are being actively searched for experimentally, but up to now have not been discovered. For discussions of current experimental constraints on the doubly charged particles and of the sensitivities to them of future experiments see [21–27] and references therein.

In addition to interesting particle-physics phenomenology, doubly charged scalars may have important implications for cosmology. In this paper we will, however, consider another aspect of their possible existence. As we shall demonstrate, doubly charged particles can catalyze fusion of light nuclei, with potentially important applications for energy production. The negatively charged  $X^{--}$  (which we will hereafter simply refer to as  $X$ ) can form atomic bound systems with the nuclei of light elements, such as deuterium, tritium, or helium. One example is the anti-helium-like ( $ddX$ ) atom with the  $X$  particle as the “nucleus” and two deuterons in the  $1s$  atomic state instead of two positrons. (Here and below we use the brackets to denote states bound by the Coulomb force). As  $X$  is expected to be very heavy, the size of such an atomic

\*akhmedov@mpi-hd.mpg.de

Published by the American Physical Society under the terms of the [Creative Commons Attribution 4.0 International license](https://creativecommons.org/licenses/by/4.0/). Further distribution of this work must maintain attribution to the author(s) and the published article’s title, journal citation, and DOI. Funded by SCOAP<sup>3</sup>.

system will in fact be determined by the deuteron mass  $m_d$  and will be of the order of the Bohr radius of the  $(dX)$  ion,  $a_d \simeq 7.2$  fm. Similar small-size atomic systems  $(NN'X)$  can exist for other light nuclei  $N$  and  $N'$  with charges  $Z \leq 2$ .

Atomic binding of two nuclei to an  $X$  particle brings them so close together that this essentially eliminates the necessity for them to overcome the Coulomb barrier in order to undergo fusion. The exothermic fusion reactions can then occur unhindered and do not require high temperature or pressure. The  $X$  particle is not consumed in this process and can then facilitate further nuclear fusion reactions, acting thus as a catalyst.

This  $X$ -catalyzed fusion mechanism is to some extent similar to muon-catalyzed fusion ( $\mu$ CF) ([28–35], see [36–42] for reviews), in which the role of the catalyst is played by singly negatively charged muons.  $\mu$ CF of hydrogen isotopes was once considered a prospective candidate for cold fusion. However, already rather early in its studies it became clear that  $\mu$ CF suffers from a serious shortcoming that may prevent it from being a viable mechanism of energy production. In the fusion processes, isotopes of helium are produced, and there is a chance that they will capture on their atomic orbits the negative muons present in the final state of the fusion reactions. Once this happens, muonic ions ( ${}^3\text{He}\mu$ ) or ( ${}^4\text{He}\mu$ ) are formed, which, being positively charged, cannot catalyze further fusion reactions. This effect is cumulative; the sticking to helium nuclei thus eventually knocks the muons out from the catalytic process, i.e., the catalytic poisoning occurs.

Out of all  $\mu$ CF reactions, the  $d-t$  fusion has the smallest muon sticking probability,  $\omega_s \simeq 10^{-2}$ . This means that a single muon will catalyze  $\sim 100$  fusion reactions before it gets removed from the catalytic process. The corresponding total produced energy is  $\sim 1.7$  GeV, which is at least a factor of 5 smaller than the energy needed to produce and handle one muon [32]. In addition, the muon's short lifetime makes it impractical to try to dissolve the produced ( ${}^3\text{He}\mu$ ) or ( ${}^4\text{He}\mu$ ) bound states by irradiating them with particle beams in order to reuse the released muons. These considerations have essentially killed the idea of using  $\mu$ CF for energy production.

There were discussions in the literature of the possibility of energy generation through the catalysis of nuclear fusion by hypothetical heavy long-lived or stable singly charged [34,43–45] or fractionally charged [46] particles. However, it has been shown in [34,44,45] that these processes suffer from the same problem of catalytic poisoning as  $\mu$ CF, and therefore they cannot be useful sources of energy. In particular, in Ref. [44] it was demonstrated that reactivation of the catalyst particles by irradiating their atomic bound states with helium nuclei by neutron beams, as suggested in [46], would require beams that are about 9 orders of magnitude higher than those currently produced by the most powerful nuclear reactors.

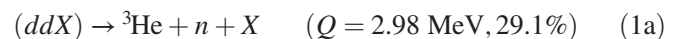
In this paper we consider the fusion of light nuclei catalyzed by doubly negatively charged  $X$  particles and demonstrate that, unlike  $\mu$ CF, this process may be a viable source of energy. We analyze  $X$ -catalyzed fusion (XCF) in deuterium environments and show that the catalytic poisoning may only occur in this case due to the sticking of  $X$  particles to  ${}^6\text{Li}$  nuclei, which are produced in the fusion reactions of the third stage. The corresponding sticking probability is shown to be very low, and, before getting bound to  ${}^6\text{Li}$ , each  $X$  particle can catalyze  $\sim 3.5 \times 10^9$  fusion cycles, producing  $\sim 7 \times 10^4$  TeV of energy. To the best of the present author's knowledge, nuclear fusion catalyzed by doubly charged particles has never been considered before.

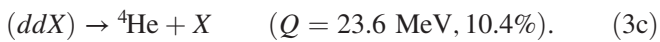
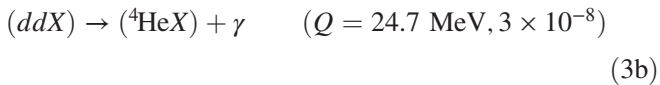
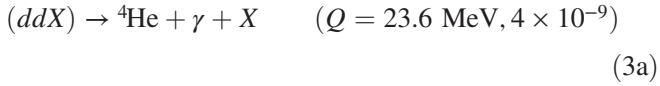
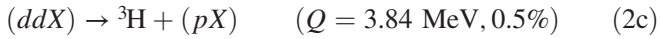
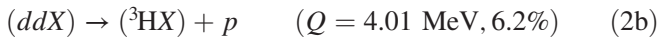
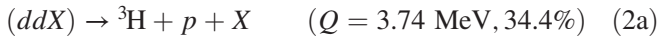
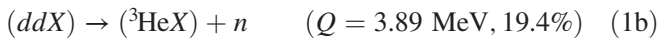
## II. X-CATALYZED FUSION IN DEUTERIUM

We will be assuming that  $X$  particles interact only electromagnetically, which in any case should be a very good approximation at low energies relevant to nuclear fusion. Let  $X$  particles be injected in pressurized  $\text{D}_2$  gas or liquid deuterium. Being very heavy and negatively charged, the  $X$  particles can easily penetrate  $\text{D}_2$  molecules and D atoms, dissociating the former and ionizing the latter and losing energy on the way. Once the velocity of an  $X$  particle becomes comparable to atomic velocities ( $v \simeq 2e^2/\hbar \sim 10^{-2}c$ ), it captures a deuteron on a highly excited atomic level of the  $(dX)$  system, which then very quickly deexcites to its ground state, mostly through electric dipole radiation and inelastic scattering on the neighboring deuterium atoms. As the  $(dX)$  ion is negatively charged, it swiftly picks up another deuteron to form the  $(ddX)$  atom. The characteristic time of this atomic phase of the XCF process is dominated by the  $X$  moderation time and is  $\sim 10^{-10}$  s at liquid hydrogen density  $N_0 = 4.25 \times 10^{22}$  nuclei/cm<sup>3</sup> and  $T \simeq 20$  K and about  $10^{-7}$  s in deuterium gas at  $0^\circ\text{C}$  and pressure of one bar (see Appendix A).

After the  $(ddX)$  atom has been formed, the deuterons undergo nuclear fusion through several channels, see below. Simple estimates show that the fusion rates are many orders of magnitude faster than the rates of the atomic formation processes. That is, once  $(ddX)$  [or similar  $(NN'X)$ ] atoms are formed, the fusion occurs practically instantaneously. The time scale of XCF is therefore determined by the atomic formation times. The rates of the fusion reactions, however, determine the branching ratios of various fusion channels, which are important for the kinetics of the catalytic cycle.

At the first stage of XCF in deuterium two deuterons fuse to produce  ${}^3\text{He}$ ,  ${}^3\text{H}$ , or  ${}^4\text{He}$ . In each case there is at least one channel in which the final-state  $X$  forms an atomic bound state with one of the produced nuclei. Stage I fusion reactions are





Here in the parentheses the  $Q$  values and the branching ratios of the reactions are shown. In evaluating the  $Q$  values we have taken into account that the atomic binding of the two deuterons to  $X$  in the initial state reduces  $Q$ , whereas the binding to  $X$  of one of the final-state nuclei increases it. As the Bohr radii of most of the  $X$ -atomic states we consider are either comparable to or smaller than the nuclear radii, in calculating the Coulomb binding energies one has to allow for the finite nuclear sizes. We do that by making use of a variational approach, as described in Appendix A 2.

The rates of reactions (1b), (2b), (2c), and (3b) with bound  $X$  particles in the final states are proportional to the corresponding  $X$ -particle sticking probabilities,  $\omega_s$ . The existence of such channels obviously affects the branching ratios of the analogous reactions with free  $X$  in the final states.

Radiative reactions (3a) and (3b) have tiny branching ratios, which are related to their electromagnetic nature and to the fact that for their  $X$ -less version,  $d + d \rightarrow {}^4\text{He} + \gamma$ , transitions of the E1 type are strictly forbidden. This comes about because the two fusing nuclei are identical, which, in particular, means that they have the same charge-to-mass ratio. This reaction therefore proceeds mainly through E2 transitions [35]. When the deuterons are bound to  $X$ , the strict prohibition of E1 transitions is lifted due to possible transitions through intermediate excited atomic states. However, as shown in Appendix A 3 b, the resulting E1 transitions are in this case heavily hindered and their rates actually fall below the rates of the E2 transitions.

Reaction (3c) is an internal conversion process. Note that, unlike for reactions (1a)–(3b), the  $X$ -less version of (3c) does not exist: the process  $d + d \rightarrow {}^4\text{He}$  is forbidden by kinematics. For the details of the calculation of the rate of reaction (3c) as well as of the rates of the other reactions discussed in this paper, see Appendix B. The relevant  $Q$

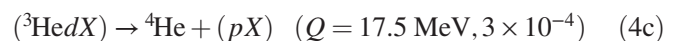
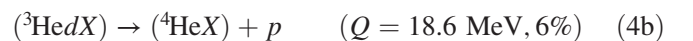
values of the reactions and sticking probabilities are evaluated in Appendices A 2 and A 3, respectively.

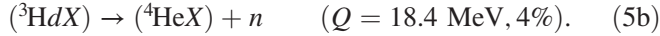
The final states of reactions (1a), (2a), (3a), and (3c) contain free  $X$  particles which are practically at rest and can immediately capture deuterons of the medium, forming again the  $(ddX)$  atoms. Thus, they can again catalyze  $d - d$  fusion through stage I reactions (1a)–(3c). The same is also true for the  $X$  particles in the final state of reaction (2c) which emerge being bound to protons. Collisions of  $(pX)$  with deuterons of the medium lead to fast replacement of the protons by deuterons through the exothermic charge exchange reaction  $(pX) + d \rightarrow (dX) + p$  with the energy release  $\sim 90$  keV (see Appendix A 1 b). The produced  $(dX)$  ion then picks up a deuteron to form the  $(ddX)$  atom, which can again participate in stage I reactions (1a)–(3c).

The situation is different for the  $X$  particles in the final states of reactions (1b) and (2b) forming the bound states with  ${}^3\text{He}$  and  ${}^3\text{H}$ , respectively. They can no longer directly participate in stage I  $d - d$  fusion reactions. However, they are not lost for the fusion process: the produced  $({}^3\text{He}X)$  and  $({}^3\text{HX})$  can still pick up deuterons of the medium to form the atomic bound states  $({}^3\text{He}dX)$  and  $({}^3\text{H}dX)$ , which can give rise to stage II fusion reactions, which we will consider next.

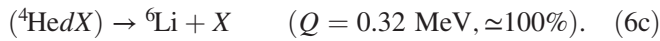
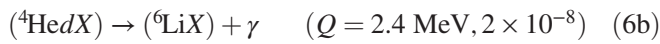
Before we proceed, a comment is in order. While  $({}^3\text{HX})$  is a singly negatively charged ion which can obviously pick up a positively charged deuteron to form an  $({}^3\text{H}dX)$  atom,  $({}^3\text{He}X)$  is a neutral  $X$  atom. It is not immediately obvious whether it can form a stable bound state with  $d$ , which, if it exists, would be a positive ion. In the case of the usual atomic systems, analogous (though negatively charged) states do exist—a well-known example is the negative ion of hydrogen  $\text{H}^-$ . However, the stability of  $({}^3\text{He}dX)$  cannot be directly deduced from the stability of  $\text{H}^-$ : in the latter case the two particles orbiting the nucleus are identical electrons, whereas for  $({}^3\text{He}dX)$  these are different entities—nuclei with differing masses and charges. Nevertheless, from the results of a general analysis of three-body Coulomb systems carried out in [47–49], it follows that the state  $({}^3\text{He}dX)$  [as well as the bound state  $({}^4\text{He}dX)$  which we will discuss later on] should exist and be stable. For additional information see Appendix 1 c.

Once  $({}^3\text{He}X)$  and  $({}^3\text{HX})$ , produced in reactions (1b) and (2b), have picked up deuterons from the medium and formed the atomic bound states  $({}^3\text{He}dX)$  and  $({}^3\text{H}dX)$ , the following stage II fusion reactions occur:





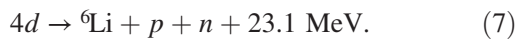
In these reactions, the vast majority of  $X$  bound to  ${}^3\text{He}$  and  ${}^3\text{H}$  are liberated; the freed  $X$  particles can again form ( $ddX$ ) states and catalyze stage I fusion reactions (1a)–(3c). The same applies to the final-state  $X$  particles bound to protons, as was discussed above. The remaining relatively small fraction of  $X$  particles come out of stage II reactions in the form of ( ${}^4\text{He}X$ ) atoms. Together with a very small amount of ( ${}^4\text{He}X$ ) produced in reaction (3b), they pick up deuterons from the medium and form ( ${}^4\text{Hed}X$ ) states, which undergo stage III XCF reactions:



In these reactions, almost all previously bound  $X$  particles are liberated and are free to catalyze nuclear fusion again through XCF reactions of stages I and II. The remaining tiny fraction of  $X$  particles end up being bound to the produced  ${}^6\text{Li}$  nuclei through reaction (6b). However, as small as it is, this fraction is very important for the kinetics of XCF. The bound states ( ${}^6\text{Li}X$ ) are ions of charge  $+1$ ; they cannot form a bound state with positively charged nuclei and participate in further XCF reaction. That is, with their formation, catalytic poisoning occurs and the catalytic process stops.

From the branching ratios of stages I, II, and III XCF reactions, one finds that the fraction of the initially injected  $X$  particles that end up in the ( ${}^6\text{Li}X$ ) bound state is  $\sim 2.8 \times 10^{-10}$ . This means that each initial  $X$  particle, before getting stuck to a  ${}^6\text{Li}$  nucleus, can catalyze  $\sim 3.5 \times 10^9$  fusion cycles.

Direct inspection shows that, independently of which subchannels were involved, the net effect of stages I, II, and III XCF reactions is the conversion of four deuterons to a  ${}^6\text{Li}$  nucleus, a proton, and a neutron:



Therefore, each initial  $X$  particle will produce about  $7 \times 10^4$  TeV of energy before it gets knocked out of the catalytic process. It should be stressed that this assumes that the  $X$  particles are sufficiently long lived to survive during  $3.5 \times 10^9$  fusion cycles. From our analysis it follows that the slowest processes in the XCF cycle are the formation of positive ions ( ${}^3\text{Hed}X$ ) and ( ${}^4\text{Hed}X$ ). The corresponding formation times are estimated to be of the order of  $10^{-8}$  s. (see Appendix A 1 c). Therefore, for the  $X$  particles to

survive during  $3.5 \times 10^9$  fusion cycles and produce  $\sim 7 \times 10^4$  TeV of energy, their lifetime  $\tau_X$  should exceed  $\sim 10^2$  s. For shorter lifetimes the energy produced by a single  $X$  particle before it gets stuck to a  ${}^6\text{Li}$  nucleus is reduced accordingly.

### III. ACQUISITION AND REACTIVATION OF $X$ PARTICLES

The amount of energy produced by a single  $X$  particle has to be compared with energy expenditures related to its production.  $X$  particles can be produced in pairs in accelerator experiments, either in  $l^+l^-$  annihilation at lepton colliders or through the Drell-Yan processes at hadronic machines. Although the energy  $E \sim 7 \times 10^4$  TeV produced by one  $X$  particle before it gets knocked out of the catalytic process is quite large on a microscopic scale, it is only about 10 mJ. This means that  $\gtrsim 10^8$   $X$  particles are needed to generate 1 MJ of energy. While colliders are better suited for the discovery of new particles, for the production of large numbers of  $X$  particles fixed-target accelerator experiments are more appropriate. For such experiments the beam energy must exceed the mass of the  $X$  particle significantly. Currently, plans for building such machines are being discussed [50].

The problem is, however, that the  $X$  particle production cross section is very small. This comes about because of their expected large mass ( $m_X \gtrsim 1 \text{ TeV}/c^2$ ) and the fact that for their efficient moderation needed to make the formation of ( $dX$ ) atoms possible,  $X$  particles should be produced with relatively low velocities. The cross section  $\sigma_p$  of the production of  $X$  particles with mass  $m_X \simeq 1 \text{ TeV}/c^2$  and  $\beta = v/c \simeq 0.3$  is only  $\sim 1$  fb (note that for scalar  $X$  particles  $\sigma_p \propto \beta^3$ ). As a result, the energy spent on production of an  $X^{++}X^{--}$  pair will be by far larger than the energy that can be generated by one  $X^{--}$  before it gets bound to a  ${}^6\text{Li}$  nucleus. This means that reactivating and reusing the bound  $X$  particles multiple times would be mandatory in this case. This, in turn, implies that only very long-lived  $X$  particles with  $\tau_X \gtrsim 3 \times 10^4$  yr will be suitable for energy production.

Reactivation of  $X$  particles bound to  ${}^6\text{Li}$  requires dissociation of ( ${}^6\text{Li}X$ ) ions. This could be achieved by irradiating them with particle beams, similarly to what was suggested for reactivation of the lower-charge catalyst particles in Ref. [46]. However, it would be much more efficient to use instead ( ${}^6\text{Li}X$ ) ions as projectiles and irradiate a target with their beam.

The Coulomb binding energy of  $X$  to  ${}^6\text{Li}$  is about 2 MeV; to strip them off by scattering on target nuclei with the average atomic number  $A \simeq 40$  one would have to accelerate ( ${}^6\text{Li}X$ ) ions to velocities  $\beta \simeq 0.01$  which, for  $m_X \simeq 1 \text{ TeV}/c^2$ , corresponds to beam energy  $\sim 0.05$  GeV. At these energies the cross section of the stripping reaction is  $\gtrsim 0.1$  b, and  $X$  particles can be liberated with high efficiency

in relatively small targets. The energy spent on the reactivation of one  $X$  particle will then only be about  $10^{-9}$  of the energy it can produce before sticking to a  ${}^6\text{Li}$  nucleus.

If  $X$  particles are stable or practically stable, i.e., their lifetime  $\tau_X$  is comparable to the age of the Universe, there may exist a terrestrial population of relic  $X$  particles bound to nuclei or (in the case of  $X^{++}$ ) to electrons and thus forming exotic nuclei or atoms. The possibility of the existence of exotic bound states containing charged massive particles was suggested in Ref. [51] (see also [52]) and has been studied by many authors. The concentration of such exotic atoms on the Earth may be very low if reheating after inflation occurs at sufficiently low temperatures. Note that reheating temperatures as low as a few MeV are consistent with observations [53]. A number of searches for such superheavy exotic isotopes has been carried out using a variety of experimental techniques, and upper limits on their concentrations were established; see [54] for a review.

Exotic helium atoms ( $X^{++}ee$ ) were searched for in the Earth's atmosphere using a laser spectroscopy technique, and the limit of their concentration  $10^{-12}$ – $10^{-17}$  per atom over the mass range  $20$ – $10^4$  GeV/ $c^2$  was established [55]. In the case of doubly negatively charged  $X$ , their Coulomb binding to nuclei of charge  $Z$  would produce superheavy exotic isotopes with nuclear properties of the original nuclei but chemical properties of atoms with nuclear charge  $Z - 2$ . Such isotopes could have accumulated in continental crust and marine sediments. Singly positively charged ions ( ${}^6\text{Li}X$ ) and ( ${}^7\text{Li}X$ ) chemically behave as superheavy protons; they can capture electrons and form anomalously heavy hydrogen atoms. Experimental searches for anomalous hydrogen in normal water have put upper limits on its concentration at the level of  $\sim 10^{-28}$ – $10^{-29}$  for the mass range 12 to 1200 GeV/ $c^2$  [56] and  $\sim 6 \times 10^{-15}$  for the masses between 10 and  $10^5$  TeV/ $c^2$  [57].

If superheavy isotopes containing relic  $X$  particles of cosmological origin exist, they can be extracted from minerals, e.g., by making use of mass spectrometry techniques, and their  $X$  particles can then be stripped off. To estimate the required energy, we conservatively assume that it is twice the energy needed to vaporize the matter sample. As an example, it takes about 10 kJ to vaporize 1 g of granite [58]; denoting the concentration of  $X$  particles in granite (number of  $X$  per molecule) by  $c_X$ , we find that the energy necessary to extract one  $X$  particle is  $\sim 2.3 \times 10^{-18}$  J/ $c_X$ . Requiring that it does not exceed the energy one  $X$  particle can produce before getting stuck to a  ${}^6\text{Li}$  nucleus leads to the constraint  $c_X \gtrsim 2.3 \times 10^{-16}$ . If it is satisfied, extracting  $X$  particles from granite would allow XCF to produce more energy than it consumes, even without reactivation and recycling of the  $X$  particles. Another advantage of the extraction of relic  $X$  particles from minerals compared with their production at accelerators is

that it could work even for  $X$  particles with mass  $m_X \gg 1$  TeV/ $c^2$ .

In assessing the viability of XCF as a mechanism of energy generation, in addition to pure energy considerations, one should obviously address many technical issues related to its practical implementation, such as collection and moderation of the produced  $X$  particles and prevention of their binding to the surrounding nuclei (or their liberation if such binding occurs), etc. However, the corresponding technical difficulties seem to be surmountable [59].

#### IV. DISCUSSION

There are several obvious ways in which our analysis of XCF can be generalized. Although we only considered nuclear fusion catalyzed by scalar  $X$  particles, doubly charged particles of nonzero spin can do the job as well. While we studied XCF in deuterium, fusion processes with participation of other hydrogen isotopes can also be catalyzed by  $X$  particles.

We considered XCF taking place in  $X$ -atomic states. The catalyzed fusion can also proceed through in-flight reactions occurring, e.g., in  $d + (dX)$  collisions. However, because even at the highest attainable densities the average distance  $\bar{r}$  between deuterons is much larger than it is in  $(ddX)$  atoms, the rates of in-flight reactions are suppressed by a factor of the order of  $(\bar{r}/a_d)^3 \gtrsim 10^9$  compared with those of reactions occurring in  $X$  atoms.

Our results depend sensitively on the properties of positive ions ( ${}^3\text{He}dX$ ) and ( ${}^4\text{He}dX$ ), for which we obtained only crude estimates. More accurate calculations of these properties and of the formation times of these positive ions would be highly desirable.

The existence of long-lived doubly charged particles may have important cosmological consequences. In particular, they may form exotic atoms, which have been discussed in connection with the dark matter problem [60–62]. They may also affect primordial nucleosynthesis in an important way. In Ref. [63] it was suggested that singly negatively charged heavy metastable particles may catalyze nuclear fusion reactions at the nucleosynthesis era, possibly solving the cosmological lithium problem. The issue has been subsequently studied by many authors; see Refs. [64,65] for reviews. Doubly charged scalars  $X$  may also catalyze nuclear fusion reactions in the early Universe and thus may have significant impact on primordial nucleosynthesis. On the other hand, cosmology may provide important constraints on the XCF mechanism discussed here. Therefore, a comprehensive study of cosmological implications of the existence of  $X^{\pm\pm}$  particles would be of great interest.

To conclude, we have demonstrated that long-lived or stable doubly negatively charged scalar particles  $X$ , if they exist, can catalyze nuclear fusion and provide a viable source of energy. Our study gives a strong additional

motivation for continuing and extending the experimental searches for such particles.

### ACKNOWLEDGMENTS

The author is grateful to Manfred Lindner, Alexei Smirnov, and Andreas Trautner for useful discussions. Special thanks are due to Maxim Pospelov for numerous helpful discussions of various aspects of  $X$ -catalyzed fusion and for constructive criticism.

*Note added.*—Recently, the ATLAS Collaboration has reported a  $3.6\sigma$  ( $3.3\sigma$ ) local (global) excess of events with large specific ionization energy loss  $|dE/dx|$  in their search for long-lived charged particles at LHC [66]. In the complete LHC Run 2 dataset, seven events were found for which the values of  $|dE/dx|$  were in tension with the time-of-flight velocity measurements, assuming that the corresponding particles were of unit charge. It has been shown in [67] that this excess could be explained as being due to relatively long-lived doubly charged particles. It would be very interesting to see if the reported excess will survive with increasing statistics of the forthcoming LHC Run 3.

## APPENDIX A: ATOMIC PROCESSES AND $X$ -ATOM FORMATION TIMES

### 1. Formation times of $X$ -atomic systems

#### a. Formation of $(dX)$ ions and of $(ddX)$ and $({}^3\text{Hd}X)$ atoms

Moderation of muons in medium and formation of  $\mu$  atoms were considered in the classic papers [68,69] which stood the test of time (see, e.g., [70]). The moderation time is practically independent of the mass of the ionizing particle and is inversely proportional to square of its charge; this allows one to deduce the moderation times for  $X$  particles by a simple scaling of the muonic case. From the results of Ref. [69] we find that the moderation time of  $X$  particles from  $\beta \equiv v/c \simeq 0.1$  to atomic velocities  $v \simeq 2e^2/\hbar \simeq 1.5 \times 10^{-2}c$  is

$$\tau \simeq 6 \times 10^{-11} \text{ s} \quad (\text{A1})$$

at liquid hydrogen density  $N_0 = 4.25 \times 10^{22}$  nuclei/cm<sup>3</sup> and  $T \simeq 20$  K. It is about  $4.8 \times 10^{-8}$  s in deuterium gas at 0° C and pressure of one bar.

Once an  $X$  particle has slowed down to atomic velocities, it gets captured on a highly excited state of the  $(dX)$  ion, which then deexcites through a combination of  $\gamma$ -ray cascade emission (mostly E1 transitions) and inelastic scattering on the neighboring deuterium atoms with their Auger ionization. This is similar to deexcitation of highly excited  $(\mu d)$  atoms in the case of  $\mu\text{CF}$ . In the latter case, the two deexcitations processes are generically of comparable

rates; at liquid hydrogen density the Auger process slightly dominates. The deexcitation to the  $(\mu d)$  ground state occurs within  $t \sim 10^{-12}$  s [71].

In the case of  $(dX)$  deexcitation, the radiative processes get enhanced. Indeed, the rates of E1 emission are proportional to cube of the energy  $E_\gamma$  of the emitted  $\gamma$  and square of the transition matrix element of the electric dipole operator  $d_{fi}$ . It is easy to see that  $E_\gamma$  scales linearly with the mass of the atomic orbiting particle  $m$ , whereas  $d_{fi}$  scales linearly with the Bohr radius of the system, i.e., is inversely proportional to  $m$ . Therefore, the rates of E1 transitions scale linearly with  $m$ . As a result, we find that the rate of radiative deexcitation of the  $(Xd)$  system is larger than that of the  $(d\mu)$  atom by a factor  $m_d/m_\mu \sim 20$ . One can therefore expect the deexcitation of  $(dX)$  ions to be at least as fast as that for the muonic deuterium, i.e., to occur within  $\sim 10^{-12}$  s.

The produced negative ion  $(dX)$  can pick up another deuteron from the medium to form a highly excited state of the  $(ddX)$  atom, which can deexcite through the same processes as  $(dX)$ . In addition, being electrically neutral,  $(ddX)$  can penetrate deep inside the neighboring deuterium atoms and experience the electric field of their nuclei. This leads to Stark mixing effects which further accelerate the de-excitation processes [71,72].

The situation is quite similar for the formation time of  $({}^3\text{Hd}X)$  atoms. An  $({}^3\text{HX})$  negative ion produced in reaction (2b) picks up a deuteron from the medium to form a highly excited state of the  $({}^3\text{Hd}X)$  atom. The latter then deexcites as described above for the  $(ddX)$  atom, within approximately the same time interval.

#### b. Charge exchange reaction $d + (pX) \rightarrow (dX) + p$

A simple and accurate estimate of the cross section of the muon exchange reaction  $d + (p\mu) \rightarrow (d\mu) + p$ , based on dimensional analysis and the fact that low-energy cross sections of inelastic processes are inversely proportional to the relative velocities of the colliding particles, was given in [36]. The cross section of the reaction  $d + (pX) \rightarrow (dX) + p$  can be estimated similarly, which yields

$$\sigma_c \simeq 4\pi a_p^2 f v_*/v. \quad (\text{A2})$$

Here  $a_p = \hbar/(2am_p c) = 1.44 \times 10^{-12}$  cm is the Bohr radius of the  $(pX)$  atom,  $v$  and  $v_*$  are the relative velocities of the involved particles in the initial and final states, respectively, and  $f$  is a constant of order unity. Taking into account that the relative velocities of the initial-state particles are very small and the  $Q$  value of the reaction  $d + (pX) \rightarrow (dX) + p$  is  $\simeq 90$  keV, we find  $v_* \simeq 1.4 \times 10^{-2}c$ , which gives

$$\sigma_c v \simeq 10^{-14} \text{ cm}^3/\text{s}. \quad (\text{A3})$$

For the rate  $\lambda_c$  and the characteristic time  $t_c$  of this reaction we then find, at liquid hydrogen density  $N_0 = 4.25 \times 10^{22}$  nuclei/cm<sup>3</sup>,

$$\lambda_c = \sigma_c v N_0 \simeq 4 \times 10^8 \text{ s}^{-1}, \quad t_c = \lambda_c^{-1} \simeq 2.5 \times 10^{-9} \text{ s}. \quad (\text{A4})$$

### c. Positive ions (<sup>3</sup>HedX) and (<sup>4</sup>HedX) and time scales of their formation

The complexes (<sup>3</sup>HedX) and (<sup>4</sup>HedX) are positive ions. Such systems can be considered as composed of a tightly bound “inner core”, represented by a neutral (HeX) atom, and a deuteron, weakly bound to the core by atomic polarization effects. The neutral atoms in the inner cores are slightly perturbed by the presence of an external deuteron and are characterized by the binding energies and Bohr radii approximately equal to those of the corresponding (<sup>3</sup>HeX) or (<sup>4</sup>HeX) atoms in the absence of the additional deuteron. The extraneous deuteron is bound on a  $1s'$  orbit characterized by a larger radius and much smaller binding energy.

It is not immediately obvious if such exotic atomic systems are actually stable; in particular, their stability cannot be deduced from the stability of negative ion of hydrogen  $\text{H}^-$  familiar from the usual atomic physics. Stability of three-body Coulomb systems with arbitrary masses and charges of the particles was studied in a number of papers, see, e.g., [47–49]. From their general results it follows that the states (<sup>3</sup>HedX) and (<sup>4</sup>HedX) should actually be stable. This can be seen from Fig. 8 of Ref. [47], Fig. 3 of [48] or Fig. 13 of [49], where the stability regions are shown in the case of arbitrary fixed masses of the particles and the charge  $q_1 = 1$  as a function of  $q_2^{-1}$  and  $q_3^{-1}$ . Here  $q_1$  is the absolute value of the charge of the particle which is opposite to the other two ( $q_1 = Z_X e$  in the case we consider), whereas  $q_2$  and  $q_3$  are the charges of the same-sign particles, with the convention  $q_2 \geq q_3$ . As the stability depends on the ratios of the charges and not on their absolute values,  $q_1$  was set equal to unity for convenience. With such a normalization, we have  $q_2 = 1$ ,  $q_3 = 1/2$ . It can be seen from the above mentioned Figures that the point  $(q_2^{-1}, q_3^{-1}) = (1, 2)$  is inside the stability region, that is, positive ions (<sup>3</sup>HedX) and (<sup>4</sup>HedX) must be stable. This point is, however, rather close to the border of the stability region, which reflects the relative smallness of the binding energy of the deuteron (“deuteron affinity”).

We have attempted a variational calculation of the binding energies of such positive ions using simple two- and three-parameter Hylleraas-type trial wave functions which were able to predict the stability of the  $\text{H}^-$  ion, but found no binding of deuteron. This is apparently related to the fact that (HedX) ions, which have nuclei of differing mass and charge on their atomic orbits, are more complex than  $\text{H}^-$  ions, whose two electrons are identical particles.

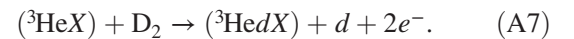
A qualitative analysis of the properties of such systems would therefore necessitate calculations with more sophisticated trial wave functions. This would require a dedicated study, which is beyond the scope of the present paper.

In the absence of an actual calculation, we have to resort to semi-quantitative methods. In doing that, we will be using the properties of a negative ion  $\text{H}^-$  as a starting point, but will also take into account the peculiarities of (<sup>3</sup>HedX) and (<sup>4</sup>HedX) ions. In the case of  $\text{H}^-$ , the radius of the outer electron’s orbit is about a factor 3.7 larger than that of the inner electron [73], and the binding energy of the outer electron (electron affinity) is about 18 times smaller than that of the inner one. Taking into account tighter binding of the inner core in the case of the positive ions we consider, we assume the radii  $a$  of their external orbits and the deuteron binding energies  $E_{bd}$  to be, respectively, a factor of  $\sim 30$  larger and 3 orders of magnitude smaller than those of the corresponding (HeX) atoms. A factor  $\sim 30$  increase for  $a$  compared with the inner core radius is obtained as follows: we multiply the factor 3.7 hinted by  $\text{H}^-$  ions by  $2 \times 2 = 4$  due to the  $X$  particle and the He nucleus each having charge 2 and by the ratio of the mass of <sup>3</sup>He (or <sup>4</sup>He) to the deuteron mass. This gives factor  $\sim 22$ –30. For the binding energy of the extra deuteron we take into account that it scales as  $a^{-2}$ . We therefore choose

$$(^3\text{HedX}): a \simeq 7 \times 10^{-12} \text{ cm}, \quad E_{bd} \simeq 1.2 \text{ keV}, \quad (\text{A5})$$

$$(^4\text{HedX}): a \simeq 5 \times 10^{-12} \text{ cm}, \quad E_{bd} \simeq 1.6 \text{ keV}. \quad (\text{A6})$$

The formation of (<sup>3</sup>HedX) and (<sup>4</sup>HedX) ions can proceed as follows. An (<sup>3</sup>HeX) atom produced in reaction (1b) collides with the neighboring  $\text{D}_2$  molecules, dissociating them and picking up one of their deuterons through the exothermic reaction



This is the dissociative attachment (DA) mechanism, analogous to the one by which  $\text{H}^-$  ions are produced in  $e^- + \text{H}_2 \rightarrow \text{H}^- + \text{H}$  reactions. An important difference is, however, that what is attached is now a nucleus (deuteron) rather than an electron. The formation of (<sup>4</sup>HedX) ions from (<sup>4</sup>HeX) atoms produced in reactions (4b) and (5b) proceeds similarly. [Note that a tiny fraction of (<sup>4</sup>HedX) ions is produced directly in the stage I reaction (3b).]

As the  $Q$  values of the formation reactions of (<sup>3</sup>HedX) and (<sup>4</sup>HedX) ions are about 2 orders of magnitude larger than the dissociation energy of  $\text{D}_2$  molecules and the ionization potential of D atoms, these processes are actually similar to the usual charge exchange reactions on free particles, except that most of the released energy is now carried away by the final-state electrons. The rates and characteristic times of these processes can therefore be estimated using the expressions similar to those in

Eqs. (A3) and (A4). This gives, at the liquid hydrogen density,

$$\lambda_{\text{DA}} \sim 5 \times 10^7 \text{ s}^{-1}, \quad t_{\text{DA}} = \lambda_{\text{DA}}^{-1} \sim 2 \times 10^{-8} \text{ s}. \quad (\text{A8})$$

## 2. Atomic binding energies of light nuclei in $X$ atoms and $Q$ values of fusion reactions

The  $Q$  value of an XCF reaction can be found by subtracting from the  $Q$  value of the corresponding  $X$ -less reaction the atomic binding energy of the nuclei in the initial state and adding to it the binding energy of one of the produced nuclei to  $X$  in the final state, when such bound states are formed. We therefore first find the relevant binding energies.

### a. Anti-helium-like ( $ddX$ ) atom

The total binding energy of the helium atom is 79.005 eV. From this value, the binding energy of the ( $ddX$ ) atom is obtained to a very good accuracy by the simple rescaling with the factor  $m_d/m_e$ , which gives  $E_b(ddX) = 0.290$  MeV.

### b. Other $X$ atoms with Coulomb-bound light nuclei

For atomic ( $NN'X$ ) states other than ( $ddX$ ) we first consider hydrogenlike atoms ( $NX$ ) and then estimate the atomic binding energy of the additional nucleus  $N'$  ( $m > m'$  is assumed). In the limit of pointlike nuclei the

ground-state wave function  $\psi_{1s}(r)$ , the Bohr radius  $a$ , and the binding energy  $E_b^0$  of an ( $NX$ ) state are

$$\psi_{1s}(r) = \frac{1}{\sqrt{\pi a^3}} e^{-r/a}, \quad a = \frac{\hbar^2}{Z_X Z e^2 m} = \frac{1}{Z_X Z \alpha m c},$$

$$E_b^0 = |E_{1s}^0| = \frac{1}{2} (Z_X Z \alpha)^2 m c^2. \quad (\text{A9})$$

Here  $Ze$  and  $m$  are the charge and the mass of the nucleus  $N$ , and  $-Z_X e$  is the charge of the  $X$  particle ( $Z_X = 2$  in the case under discussion).

For most of the nuclei we consider that the Bohr radii of the ( $NX$ ) atomic states are either comparable to or smaller than the nuclear radii, and the approximation of pointlike nuclei is rather poor. We therefore allow for finite nuclear sizes by making use of a variational approach. We consider nuclei as uniformly charged balls of radius  $R$  and employ the simple one-parameter test wave function of Flügge and Zickendrant, which has the correct asymptotics for both large and small  $r$  [74,75]:

$$\psi(r) = N(\lambda) \left( 1 + \frac{\lambda r}{2R} \right) e^{-\frac{\lambda r}{2R}}, \quad N(\lambda) = \sqrt{\frac{1}{7\pi} \left( \frac{\lambda}{2R} \right)^3}. \quad (\text{A10})$$

Here  $\lambda$  is the variational parameter. With this wave function, the expectation value of the energy of the system is

$$E(\lambda) = \frac{3}{56} \frac{\hbar^2}{m R^2} \left\{ \lambda^2 + \frac{R}{a} \left[ \frac{216}{\lambda^2} - 28 - e^{-\lambda} \left( \frac{216}{\lambda^2} + \frac{216}{\lambda} + 80 + 14\lambda + \lambda^2 \right) \right] \right\}. \quad (\text{A11})$$

We minimize it numerically, which yields the ground-state energy  $E_{1s}$ , the binding energy of the system being  $E_b(R) = |E_{1s}|$ . The corresponding value of  $\lambda$  determines, through Eq. (A10), the ground-state wave function of the system. It will be used in the calculations of the sticking probabilities in Appendix A 3 a below.

We calculate the binding energies of ( $NX$ ) states for two different choices of the values of the nuclear radii  $R$ .

First, we employ the frequently used expression  $R = R_N \equiv 1.2A^{1/3}$  fm, where  $A$  is the atomic number of the nucleus  $N$ . Second, we make use of the experimentally measured rms charge radii  $r_{Nc} \equiv \langle r_c^2 \rangle_N^{1/2}$  [76] and set the nuclear radii equal to  $R_{Nc} \equiv (5/3)^{1/2} r_{Nc}$ , which is the relation between  $R_{Nc}$  and  $r_{Nc}$  in the uniformly charged ball model of the nucleus. The results are presented in Table I along with the Bohr radii  $a$  and

TABLE I. Properties of ( $NX$ ) bound states. Third and fifth columns show experimental values of rms charge radii  $r_{Nc} \equiv \langle r_c^2 \rangle_N^{1/2}$  from Ref. [76] and the corresponding nuclear radii found as  $R_{Nc} = (5/3)^{1/2} r_{Nc}$ .  $E_b(R_N)$  and  $E_b(R_{Nc})$  are binding energies calculated for the corresponding values of nuclear radii;  $E_b^0 = (Z_X Z \alpha)^2 m c^2 / 2$  is binding energy in the limit of pointlike nuclei.

Bound state	Bohr radius $a$ (fm)	$r_{Nc}$ (fm) [76]	$R_N = 1.2A^{1/3}$ (fm)	$R_{Nc}$ (fm)	$E_b(R_N)$ (MeV)	$E_b(R_{Nc})$ (MeV)	$E_b^0$ (MeV)
( $pX$ )	14.4	0.8783	1.20	1.134	0.096	0.096	0.100
( $dX$ )	7.20	2.142	1.51	2.765	0.189	0.183	0.200
( $^3\text{HX}$ )	4.81	1.759	1.73	2.271	0.276	0.268	0.299
( $^3\text{HeX}$ )	2.41	1.966	1.73	2.538	1.00	0.905	1.196
( $^4\text{HeX}$ )	1.81	1.676	1.905	2.163	1.202	1.153	1.588
( $^6\text{LiX}$ )	0.805	2.589	2.18	3.342	2.680	2.069	5.369



the binding energies for pointlike nuclei  $E_b^0$ . Note that for our further calculations we use the results based on the experimentally measured nuclear charge radii, which are presumably more accurate.

As a test, we also performed similar calculations for atomic systems ( $NC$ ) with  $C$  a singly negatively charged heavy particle, for which the binding energies were previously found in [63]. Our results are in good agreement with those of Ref. [63], the difference typically being within 1%.

The binding energies of the  $X$  atoms in the initial states of the XCF reactions other than ( $ddX$ ) are found as follows. For ( ${}^3\text{HdX}$ ) atoms, we add to the binding energy of the negative ( ${}^3\text{HX}$ ) ion the deuteron binding energy found through the variational procedure described above, assuming the deuteron to be a pointlike particle in the Coulomb field of a nucleus of charge  $Z_{\text{H}} - Z_X = -1$  and radius equal to that of the  ${}^3\text{H}$  nucleus. For positive ions ( ${}^3\text{HedX}$ ) and ( ${}^4\text{HedX}$ ), we add to the binding energies of ( ${}^3\text{HeX}$ ) and ( ${}^4\text{HeX}$ ) atoms the deuteron binding energy  $E_{bd}$  given in Eqs. (A5) and (A6), respectively. The obtained binding energies are then used for calculating the  $Q$  values of the XCF reactions under consideration. The results are shown in the third column of Table III.

### 3. Sticking probabilities and related issues

#### a. Sticking probabilities in the sudden approximation

To evaluate the probability  $\omega_s$  that the  $X$  particle in the final state of a fusion process will stick to one of the produced nuclear fragments, we make use of the fact that nuclear reactions of XCF occur on time scales that are much shorter than the characteristic  $X$ -atomic time. Indeed, the characteristic time of  $X$ -atomic processes is  $t_{\text{at}} \sim a_d/v_{\text{at}} \sim \hbar^3/(4m_d e^4) \simeq 1.6 \times 10^{-21}$  s, whereas the fusion reactions of XCF occur on the nuclear time scales  $\lesssim 10^{-23}$  s. This disparity between the atomic and nuclear time scales in XCF allows one to use the sudden approximation [77] for evaluating the  $X$ -sticking probabilities  $\omega_s$ .

Consider the reaction ( $N_1 N_2 X$ )  $\rightarrow N_3 + N_4 + X$ . Just before the fusion occurs, the nuclei in the ( $N_1 N_2 X$ ) atom approach each other to a distance of the order of the range of nuclear force. The atomic wave function therefore adiabatically goes over into that of the hydrogenlike atom with a nucleus of mass  $m_i = m_1 + m_2$  and charge  $Z_i = Z_1 + Z_2$  orbiting the  $X$  particle. We denote this wave function  $\psi_i$ . As the fusion occurs suddenly (compared with the atomic time scale), the state of the atomic system immediately after the fusion will be described by the same wave function. Transition amplitudes can then be found by projecting it onto the proper final states. Let the velocity of the produced nucleus  $N_3$  of mass  $m_3$  be  $\vec{v}$ . As the final-state  $X$  particle is practically at rest, this is also the relative velocity of  $N_3$  and  $X$ . The probability that  $N_3$  will get captured by  $X$  and form a bound state with it is then

$$\omega_s = \sum_{\alpha} \left| \int \psi_{f\alpha}^* \psi_i e^{-i\vec{q}\vec{r}} dV \right|^2, \quad (\text{A12})$$

where  $\psi_{f\alpha}$  is the wave function of the final ( $N_3 X$ ) state and  $\vec{q} = m_* \vec{v}/\hbar$ ,  $m_* = m_3 m_X / (m_3 + m_X) \simeq m_3$  is the reduced mass of the  $N_3 X$  system. The sum in (A12) is over all the bound states of the hydrogenlike atom ( $N_3 X$ ).

The case of radiative fusion reactions ( $N_1 N_2 X$ )  $\rightarrow N_3 + \gamma + X$  is considered quite similarly. However, due to different kinematics, the values of  $q = |\vec{q}|$  are related differently to the  $Q$  values for these reactions. For the nonradiative reactions we have  $q = \sqrt{2\mu Q}/\hbar$  with  $\mu = m_3 m_4 / (m_3 + m_4)$ , whereas for the radiative ones we have  $q \simeq Q/(\hbar c)$ .

The main contribution to  $\omega_s$  comes from the transition to the ground state of the ( $N_3 X$ ) atom, with the total contribution of all the excited states being less than 20% [34]. For our estimates we shall therefore restrict ourselves to transitions to the ground states. The functions  $\psi_i$  and  $\psi_f$  are then the wave functions of the  $1s$  states of the hydrogenlike atoms with masses and charges of the atomic particles  $m_i = m_1 + m_2$ ,  $Z_i = Z_1 + Z_2$ , and  $m_f = m_3$ ,  $Z_f = Z_3$ , respectively.

To take into account the finite size of the nuclei, we use the wave functions (A10) with the substitutions  $\lambda \rightarrow \lambda_{i,f}$ , where the variational parameters  $\lambda_{i,f}$  are found from the minimization of  $E(\lambda)$  defined in (A11) with the replacements  $a \rightarrow a_{i,f}$  and  $R \rightarrow R_{i,f}$ . The Bohr radii  $a_{i,f}$  are given by the standard formula [see Eq. (A17) below]; the nuclear radii  $R_{i,f}$  can be found from the rms nuclear charge radii as discussed in Appendix A 2 b. To find  $R_f$ , we can directly use the experimentally measured rms charge radius of the nucleus  $N_3$ . For the initial state, we approximate the rms charge radius  $r_i$  of the compound nucleus  $N_1 N_2$  as

$$r_i \simeq (r_{N_1c}^3 + r_{N_2c}^3)^{1/3}, \quad (\text{A13})$$

where  $r_{N_1c} \equiv \langle r_c^2 \rangle_{N_1}^{1/2}$  and  $r_{N_2c} \equiv \langle r_c^2 \rangle_{N_2}^{1/2}$  are the experimentally measured rms charge radii of the  $N_1$  and  $N_2$  nuclei, respectively. Note that Eq. (A13) corresponds to the liquid drop model of nucleus. Equation (A12) then gives for the sticking probability

$$\omega_s = \left[ \frac{32\pi N_i N_f \kappa}{(\kappa^2 + q^2)^3} \left( \kappa^2 + \frac{3\kappa_i \kappa_f (\kappa^2 - q^2)}{\kappa^2 + q^2} \right) \right]^2, \quad (\text{A14})$$

where

$$N_{i,f} = N(\lambda_{i,f}), \quad \kappa_{i,f} = \frac{\lambda_{i,f}}{2R_{i,f}}, \quad \kappa = \kappa_i + \kappa_f. \quad (\text{A15})$$

For comparison, we also calculate the sticking probabilities  $\omega_{s0}$  neglecting the nuclear size, i.e., employing the usual ground-state wave functions of the hydrogenlike

atoms with pointlike nuclei (A9). From Eq. (A12) we find

$$\omega_{s0} = \frac{(2a_r)^6}{(a_i a_f)^3} \frac{1}{(1 + q^2 a_r^2)^4}, \quad (\text{A16})$$

where

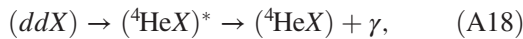
$$a_{i,f} = \frac{\hbar}{Z_X Z_{i,f} \alpha m_{i,f} c}, \quad a_r = \frac{a_i a_f}{a_i + a_f}. \quad (\text{A17})$$

The obtained values of the sticking probabilities  $\omega_s$  and  $\omega_{s0}$  are shown in the fourth and fifth columns of Table III.

### b. Lifting the prohibition of radiative E1 transitions for Coulomb-bound nuclei

The radiative nuclear fusion reaction  $d + d \rightarrow {}^4\text{He} + \gamma$  has a tiny branching ratio. This is because it proceeds mostly through E2 electromagnetic transitions, as E1 transitions are strictly forbidden for fusions of identical particles. Indeed, after the separation of the irrelevant center-of-mass motion, one finds that for particles of charges  $q_{1,2}$  and masses  $m_{1,2}$  the effective charge of the electric dipole operator is  $q = (q_1 m_2 - q_2 m_1)/(m_1 + m_2)$ , which vanishes when the two particles have the same charge-to-mass ratio.

The situation may be different for XCF, when the fusing particles are bound to an orbit of an  $X$  atom. Fusion may then proceed through the transition to an intermediate excited atomic state, which then deexcites via atomic electric dipole radiation. In this mechanism the motion of the center of mass of the initial-state nuclei plays a central role, and the effective charge of the dipole operator does not vanish. Consider the XCF reaction



where  $(ddX)$  is in its ground  $(1s)^2$  state and  $({}^4\text{HeX})^*$  is an excited state of the  $({}^4\text{HeX})$  atom which can decay through an E1 transition. For definiteness, we take  $({}^4\text{HeX})^*$  to be a state with the principal quantum number  $n = 3$  (contributions of states with higher  $n$  are in general suppressed as  $1/n^3$ ). Conservation of the total angular momentum and parity in strong interactions responsible for the fusion process imply that the intermediate  $n = 3$  state can be either  $3s$  or  $3d$ . The excited  $({}^4\text{HeX})^*$  state can then decay through E1  $\gamma$  emission to the  $2p$  state of the  $({}^4\text{HeX})$  atom, which will eventually deexcite to the ground state of  $({}^4\text{HeX})$ . Thus, the radiative fusion reaction (3b) might proceed through an E1 transition from an excited state of  $({}^4\text{HeX})$  rather than through the usual E2 transitions.

It is easy to see, however, that this does not lead to any appreciable increase of the rate of reaction (3b). Indeed, the amplitude of the process in Eq. (A18) contains the product

of the amplitude of fusion with the formation of  $({}^4\text{HeX})^*$  and the amplitude of its subsequent E1 deexcitation. The rate of the process (A18) is therefore proportional to the probability that  ${}^4\text{He}$  produced as a result of the fusion reaction is bound to  $X$  in an excited state of the  $({}^4\text{HeX})$  atom rather than being ejected. The latter can be found in the sudden approximation by making use of the expression on the right-hand side of Eq. (A12) with  $\psi_{f\alpha}$  being the wave functions of the  $3s$  and  $3d$  states. Using for our estimates the hydrogenlike wave functions for pointlike nuclei, we find for the corresponding probabilities

$$P_{3s} = \frac{2^8 (q^2 a^2)^2 (q^2 a^2 + \frac{16}{27})^2}{3^3 (q^2 a^2 + \frac{16}{9})^8}, \quad P_{3d} = \frac{2^{17} (q^2 a^2)^2}{3^9 (q^2 a^2 + \frac{16}{9})^8}. \quad (\text{A19})$$

Here  $q \simeq Q/(\hbar c)$  is the momentum transfer to the produced  ${}^4\text{He}$  nucleus divided by  $\hbar$ , and  $a$  is the Bohr radius of the  $({}^4\text{HeX})$  atom. Note that these probabilities are suppressed for both large and small  $qa$ . Large- $qa$  quenching is a result of fast oscillations of the factor  $e^{-i\vec{q}\vec{r}}$  in the integrand of (A12), whereas the suppression at small  $qa$  is a consequence of the orthogonality of the wave functions  $\psi_{f\alpha}$  and  $\psi_i$ . For process (A18) we have  $qa \simeq 0.22$ , which yields  $P_{3s} \simeq 8 \times 10^{-3}$ ,  $P_{3d} \simeq 1.1 \times 10^{-2}$ . In estimating the rate of reaction (A18) we also have to take into account that the photon emission process is nonresonant. This leads to an additional suppression by the factor  $\sim (\Delta E/E_\gamma)^2 \simeq 9 \times 10^{-5}$ , where  $\Delta E \simeq 0.2$  MeV is the energy difference between the  $n = 3$  and  $n = 2$  states of the  $({}^4\text{HeX})$  atom and  $E_\gamma \simeq Q \simeq 24$  MeV is the energy of the emitted  $\gamma$ . As a result, the rate of the  $X$ -atomic E1 transition gets suppressed by a factor  $1.7 \times 10^{-6}$  compared with what is expected for a typical E1 transition.

To assess the importance of the  $X$ -atomic channel (A18) of reaction (3b) we use the simple estimate of the rates of electric multipole transitions from Ref. [78]:

$$\Gamma(\text{E}l) \simeq \frac{2(l+1)}{l![(2l+1)!!]^2} \left(\frac{3}{l+3}\right)^2 \alpha \left(\frac{E_\gamma R}{\hbar c}\right)^{2l} \frac{E_\gamma}{\hbar}. \quad (\text{A20})$$

Here  $R$  is the nuclear radius  $R_N$  for nuclear transitions and the size of the atomic system  $a$  for transitions between atomic states. Note that, in the case of  $X$  atoms with light nuclei, the nuclear and atomic radii are of the same order of magnitude (see Table I). For the process under consideration one could expect, neglecting the suppression of E1 transitions,  $\Gamma(\text{E}1)_{\text{unsup.}}/\Gamma(\text{E}2) \sim (625/12)(E_\gamma a/\hbar c)^{-2} \sim 800$ . Taking into account the discussed above suppression factor, we arrive at  $\Gamma(\text{E}1)/\Gamma(\text{E}2) \sim 1.4 \times 10^{-3}$ .

Thus, although transitions through excited atomic states of the  $({}^4\text{HeX})$  atom lift the forbiddance of electric dipole radiation in the fusion reaction (3b), the resulting E1

transition is heavily hindered, and its contribution to the rate of the process can be neglected.

A very similar argument applies to the radiative fusion reaction (6b). Although the fusing nuclei,  ${}^4\text{He}$  and  $d$ , are not identical in this case, they have nearly the same charge-to-mass ratio. As a result, in the corresponding  $X$ -less reaction E1 transitions are heavily suppressed, and the reaction proceeds primarily through the E2 radiation. The XCF reaction (6b) could go through excited atomic states of the ( ${}^6\text{Li}X$ ) atom. We find, however, that in this case the suppression of the atomic E1 transition is even stronger than it is for reaction (3b). Indeed, the  $Q$  value of the reaction is rather small ( $Q \simeq 2.4$  MeV), leading to  $qa \simeq 10^{-2}$ . Assuming again transitions through  $n = 3$  atomic states, we find for the probabilities of formation of the excited states ( ${}^6\text{Li}X$ )\* the values  $P_{3s} \simeq 3 \times 10^{-10}$ ,  $P_{3d} \simeq 6 \times 10^{-10}$ . The suppression factor due to the non-resonant nature of the radiative transitions from the  $3s$  and  $3d$  states to the  $2p$  state of ( ${}^6\text{Li}X$ ) is  $(\Delta E/E_\gamma)^2 \simeq 0.02$ . Altogether, this gives for the atomic E1 transitions in process (6b) the suppression factor  $\sim 2 \times 10^{-11}$ , which makes them completely irrelevant.

## APPENDIX B: ASTROPHYSICAL S-FACTORS, REACTION FACTORS, AND FUSION RATES

In this section we give the details of our calculations of the cross sections, rates, and branching ratios of the XCF reactions under discussion.

### 1. Cross sections and reaction factors

The cross section of a fusion reaction of nuclei  $N_1$  and  $N_2$  of masses  $m_{1,2}$  and charges  $Z_{1,2}$  is usually written as [79]

$$\sigma(E) = \frac{S(E)}{E} e^{-2\pi\eta_{12}}, \quad (\text{B1})$$

where  $S(E)$  is the so-called astrophysical factor,  $E$  is the c.m. system energy and  $\eta_{12}$  is the Sommerfeld parameter:

$$\eta_{12} = \frac{Z_1 Z_2 e^2}{\hbar v} = Z_1 Z_2 \alpha \sqrt{\frac{\mu c^2}{2E}}, \quad \mu = \frac{m_1 m_2}{m_1 + m_2}. \quad (\text{B2})$$

Here  $v$  is the relative velocity of the fusing particles. If there are no low-energy resonances in the fusion reaction, the astrophysical factor  $S(E)$  is a slowly varying function of  $E$  at low energies. For catalyzed fusion from the relative  $s$ -wave state of  $N_1$  and  $N_2$  the reaction factor  $A(E)$  is defined as  $A(E) = \sigma(E) v C_0^{-2}$  [32]. Here  $C_0^2$  is the  $s$ -wave Coulomb barrier penetration probability factor:

$$C_0^2 = \frac{2\pi\eta_{12}}{e^{2\pi\eta_{12}} - 1}. \quad (\text{B3})$$

This gives

$$A(E) = \frac{S(E)}{\pi Z_1 Z_2 \alpha \mu c} (1 - e^{-2\pi\eta_{12}}). \quad (\text{B4})$$

The transition from  $S(E)$  to  $A(E)$  takes into account the fact that the catalyst particle screens the Coulomb fields of the fusing nuclei and essentially eliminates the Coulomb barrier. The rates  $\lambda$  of XCF reactions are related to the corresponding  $A(E)$  factors as

$$\lambda = A(E) \rho_0, \quad \rho_0 \equiv \overline{|\psi_i(0)|_R^2}. \quad (\text{B5})$$

Here  $\rho_0$  is the squared modulus of the atomic wave function of the initial ( $N_1 N_2 X$ ) state taken at zero separation between the nuclei  $N_1$  and  $N_2$  (more precisely, at a distance of the order of the range of nuclear forces) and integrated over their distance  $R$  to the  $X$  particle. It plays the same role as the number density  $n$  of the target particles in the usual expression for the reaction rates  $\lambda = \sigma n v$  [32].

In muonic molecules or molecular ions, the energies of relative motion of nuclei are very low, so that  $\eta_{12} \gg 1$ ; the term  $e^{-2\pi\eta_{12}}$  in Eq. (B4) is therefore always omitted in the literature on  $\mu\text{CF}$ . In addition, in evaluating the cross sections of the fusion reactions it is usually sufficient to consider the astrophysical  $S$  factors in the limit  $E \rightarrow 0$ .

In contrast to this, in XCF processes the kinetic energy  $E$  of the relative motion of the nuclei  $N_1$  and  $N_2$  in ( $XN_1N_2$ ) atoms is not negligible. For a system of charges bound by the Coulomb force, the virial theorem relates the mean kinetic energy  $\bar{T}$  and mean potential energy  $\bar{U}$  as  $2\bar{T} = -\bar{U}$ . Therefore, the mean kinetic energy  $\bar{T}$  in the ground state coincides with the binding energy of the system:  $E_b = |\bar{T} + \bar{U}| = \bar{T}$ . On the other hand,  $\bar{T}$  is the sum of the mean kinetic energies of the relative motion of  $N_1$  and  $N_2$  and of their center-of-mass motion. In the ( $ddX$ ) atom, these two energies are to a good accuracy equal to each other, which gives  $E \simeq E_b/2 = 0.145$  MeV. For other ( $XN_1N_2$ ) atomic systems of interest, the situation is more complicated; a rough estimate of the kinetic energy of relative motion of the fusing nuclei yields  $E \simeq E_b m_2 / (m_1 + m_2)$ , where  $m_2$  is the smaller of the two masses.

This can be explained as follows. Consider for simplicity the wave function of the ( $N_1 N_2 X$ ) atom to be a product of the hydrogenlike wave functions of ( $N_1 X$ ) and ( $N_2 X$ ) systems, i.e.,

$$\Psi_i(\vec{r}_1, \vec{r}_2) = \frac{1}{\pi(a_1 a_2)^{3/2}} e^{-\frac{r_1}{a_1} - \frac{r_2}{a_2}}. \quad (\text{B6})$$

Such a wave function occurs when one neglects the Coulomb interaction between  $N_1$  and  $N_2$ , but in fact  $\Psi_i$  of this form can partly include correlations between  $N_1$  and  $N_2$  provided that one replaces the charge of the  $X$  particle  $Z_X$  by an effective charge  $Z_{X\text{eff}}$  in the expressions for the

Bohr radii  $a_1$  and  $a_2$  or, better still, treats  $a_1$  and  $a_2$  as variational parameters. The ground-state mean values of the total kinetic energy of the  $(N_1N_2X)$  system, kinetic energy of the center of mass of  $N_1$  and  $N_2$ , and their relative kinetic energy are then

$$\begin{aligned} \bar{T} &= \frac{\hbar^2}{2m_1a_1^2} + \frac{\hbar^2}{2m_2a_2^2}, & \bar{T}_{\text{c.m.}} &= \frac{\hbar^2}{2m} \left( \frac{1}{a_1^2} + \frac{1}{a_2^2} \right), \\ \bar{T}_{\text{rel}} \equiv E &= \frac{\hbar^2}{2m_1a_1^2} \frac{m_2}{m} + \frac{\hbar^2}{2m_2a_2^2} \frac{m_1}{m}, \end{aligned} \quad (\text{B7})$$

where  $m \equiv m_1 + m_2$ . Note that  $\bar{T}_{\text{c.m.}} + \bar{T}_{\text{rel}} = \bar{T}$ . For  $m_1 = m_2$  we find  $E = \bar{T}/2 = E_b/2$ . Assume now  $m_1 > m_2$ . Since we expect  $a_i \propto m_i^{-1}$  ( $i = 1, 2$ ), the kinetic energies in Eq. (B7) can be estimated as

$$\begin{aligned} \bar{T} &\sim \frac{\hbar^2}{2m_1a_1^2}, & \bar{T}_{\text{c.m.}} &\sim \frac{\hbar^2}{2ma_1^2}, \\ E = \bar{T} - \bar{T}_{\text{c.m.}} &\sim \frac{\hbar^2}{2m_1a_1^2} \frac{m_2}{m} \sim \bar{T} \frac{m_2}{m}, \end{aligned} \quad (\text{B8})$$

which yields  $E \sim E_b m_2 / (m_1 + m_2)$ .

Wave function (B6) can also be used for evaluating the parameter  $\rho_0$  defined in Eq. (B5). Direct calculation gives

$$\rho_0 = \frac{1}{\pi(a_1 + a_2)^3}. \quad (\text{B9})$$

We shall also employ the wave function  $\Psi_i(\vec{r}_1, \vec{r}_2)$  of Eq. (B6) in Appendix B 3 for evaluating of the parameter  $\rho_1$  that enters into the expression for the rates of reactions (3c) and (6c).

## 2. Astrophysical $S$ factors and XCF reaction rates

The Coulomb binding of the fusing nuclei  $N_1$  and  $N_2$  to an  $X$  particle should have no effect on the strong interactions responsible for the fusion and can only modify the

reaction rates due to the facts that (i) the Coulomb repulsion barrier is actually eliminated due to the very close distance between  $N_1$  and  $N_2$  in the  $X$ -atom, and (ii) because of the very small size of  $X$ -atoms, the number densities of  $N_1$  and  $N_2$  within an  $(N_1N_2X)$  atom are many orders of magnitude larger than their number densities achievable for in-flight fusion. This means that, for those reactions that can occur in the absence of  $X$  particles, we can use the experimentally measured values of the corresponding astrophysical  $S$  factors in order to calculate the rates of the XCF reactions. We take the relevant data from Refs. [80–85]. For internal conversion (IC) reactions (3c) and (6c), which do not have  $X$ -less analogues, we calculate the rates directly in the next subsection. The input data necessary for the calculations of the reaction factors  $A(E)$  for all the discussed reactions and the obtained results are shown in Table II.

## 3. Rates of internal conversion (IC) processes (3c) and (6c)

IC is deexcitation of an excited nucleus in an atom through the ejection of an atomic electron (or, in the case of muonic atoms, of a muon) [86]. For IC in a process of nuclear fusion, the initial excited nuclear state is a compound nucleus formed by the merger of the two fusing nuclei. In the case of  $\mu\text{CF}$ , the ejected particle is the muon; for XCF, it is more appropriate to speak about the ejection of the final-state nucleus itself rather than of the  $X$  particle, as the latter is expected to be much heavier than light nuclei. However, when considered in terms of the relative motion between the “nucleus” and the orbiting particle, the treatment of IC in XCF closely parallels that in the case of the usual atoms or molecules.

At low energies relevant to fusion of light nuclei, IC predominantly proceeds through electric monopole (E0) transitions whenever this is allowed by angular momentum and parity selection rules. This is the case for reactions (3c) and (6c). The matrix element of an E0 transition can be written as [87]

TABLE II. Binding energies  $E_b$ , relative kinetic energies  $E$  of fusing nuclei, astrophysical  $S$ -factors  $S(E)$ , reaction factors  $A(E)$ ,  $\rho$  parameters and rates  $\lambda$  for the XCF reactions of stages I, II and III. Rates are inclusive of all subchannels with either free or bound  $X$  particles in the final state, except for IC processes, where final-state  $X$  can only be free. Symbol ” means same as in the above line.  $\rho$  factors shown in the sixth column are values of  $\rho_1$  for IC reactions (3c) and (6c) and  $\rho_0$  for all other reactions. See text for details.

Reaction	$E_b$ (MeV)	$E$ (MeV)	$S(E)$ (MeV b)	$A(E)$ (cm <sup>3</sup> /s)	$\rho_{0,1}$ (10 <sup>35</sup> cm <sup>-3</sup> )	$\lambda$ (s <sup>-1</sup> )
$(ddX) \rightarrow {}^3\text{He} + n + X$	0.290	0.145	0.102 [80]	$1.31 \times 10^{-16}$	0.64	$8.4 \times 10^{18}$
$(ddX) \rightarrow {}^3\text{H} + p + X$	”	”	$8.6 \times 10^{-2}$ [80]	$1.11 \times 10^{-16}$	”	$7.1 \times 10^{18}$
$(ddX) \rightarrow {}^4\text{He} + \gamma + X$	”	”	$7 \times 10^{-9}$ [83]	$9.0 \times 10^{-24}$	”	$5.8 \times 10^{11}$
$(ddX) \rightarrow {}^4\text{He} + X$	”	”	$1.9 \times 10^{-2}$	$2.5 \times 10^{-17}$	0.73	$1.8 \times 10^{18}$
$({}^3\text{He}dX) \rightarrow {}^4\text{He} + p + X$	0.91	0.36	7.1 [84]	$4.0 \times 10^{-15}$	$7.6 \times 10^{-3}$	$3.0 \times 10^{18}$
$({}^3\text{H}dX) \rightarrow {}^4\text{He} + n + X$	0.32	0.13	5.6 [85]	$6.2 \times 10^{-15}$	0.88	$5.5 \times 10^{20}$
$({}^4\text{He}dX) \rightarrow {}^6\text{Li} + \gamma + X$	1.16	0.39	$1.3 \times 10^{-8}$ [82]	$6.6 \times 10^{-24}$	$1.8 \times 10^{-2}$	$1.2 \times 10^{10}$
$({}^4\text{He}dX) \rightarrow {}^6\text{Li} + X$	”	”	1.55	$7.9 \times 10^{-16}$	0.14	$1.1 \times 10^{19}$

TABLE III. General characteristics of reactions (1a)–(6c).  $Q$  and  $Br$  are  $Q$  values and branching ratios of XCF reactions;  $Q_0$  and  $Br_0$  are values of these parameters for the corresponding  $X$ -less processes.  $\omega_s$  and  $\omega_{s0}$  are  $X$ -sticking probabilities found for nuclei of finite and zero radius, respectively.

Reaction	$Q_0$ (MeV)	$Q$ (MeV)	$\omega_{s0}$	$\omega_s$	$Br_0$	$Br$
$(ddX) \rightarrow {}^3\text{He} + n + X$	3.27	2.98	Not applicable	Not applicable	54.2%	29.1%
$(ddX) \rightarrow ({}^3\text{He}X) + n$	Not applicable	3.89	0.61	0.40	Not applicable	19.4%
$(ddX) \rightarrow {}^3\text{H} + p + X$	4.03	3.74	Not applicable	Not applicable	45.8%	34.4%
$(ddX) \rightarrow ({}^3\text{HX}) + p$	Not applicable	4.01	0.22	0.15	Not applicable	6.2%
$(ddX) \rightarrow {}^3\text{H} + (pX)$	Not applicable	3.84	$1.9 \times 10^{-2}$	$1.2 \times 10^{-2}$	Not applicable	0.5%
$(ddX) \rightarrow {}^4\text{He} + \gamma + X$	23.85	23.56	Not applicable	Not applicable	$3.7 \times 10^{-8}$	$4 \times 10^{-9}$
$(ddX) \rightarrow ({}^4\text{He}X) + \gamma$	Not applicable	24.71	0.95	0.87	Not applicable	$3 \times 10^{-8}$
$(ddX) \rightarrow {}^4\text{He} + X$	Not applicable	23.56	Not applicable	Not applicable	Not applicable	10.4%
$({}^3\text{He}dX) \rightarrow {}^4\text{He} + p + X$	18.35	17.44	Not applicable	Not applicable	100%	94%
$({}^3\text{He}dX) \rightarrow ({}^4\text{He}X) + p$	Not applicable	18.60	0.29	0.06	Not applicable	6%
$({}^3\text{He}dX) \rightarrow {}^4\text{He} + (pX)$	Not applicable	17.54	$2.3 \times 10^{-3}$	$3.0 \times 10^{-4}$	Not applicable	$3.0 \times 10^{-4}$
$({}^3\text{H}dX) \rightarrow {}^4\text{He} + n + X$	17.59	17.27	...	Not applicable	100%	96%
$({}^3\text{H}dX) \rightarrow ({}^4\text{He}X) + n$	Not applicable	18.42	0.23	$4.0 \times 10^{-2}$	Not applicable	4.0%
$({}^4\text{He}dX) \rightarrow {}^6\text{Li} + \gamma + X$	1.475	0.32	...	Not applicable	100%	$10^{-13}$
$({}^4\text{He}dX) \rightarrow ({}^6\text{Li}X) + \gamma$	Not applicable	2.39	$1\text{--}1.2 \times 10^{-6}$	$1\text{--}1.2 \times 10^{-3}$	Not applicable	$1.9 \times 10^{-8}$
$({}^4\text{He}dX) \rightarrow {}^6\text{Li} + X$	Not applicable	0.32	Not applicable	Not applicable	Not applicable	$\simeq 100\%$

$$M_{fi} = \frac{2\pi}{3} Z_X e^2 \tilde{Q}_0 \psi_f^*(0) \psi_i(0). \quad (\text{B10})$$

Here  $\psi_i(0)$  is the atomic wave function of the initial-state compound nucleus bound to the  $X$  particle and  $\psi_f(0)$  is the final-state continuum atomic wave function of the ejected nucleus, both taken at zero separation between the nucleus and the  $X$  particle. The quantity  $\tilde{Q}_0$  (not to be confused with  $Q_0$  of Table III) is the transition matrix element of the nuclear charge radius operator between the initial and final nuclear states:

$$\tilde{Q}_0 = \langle f | \sum_{i=1}^Z r_{pi}^2 | i \rangle. \quad (\text{B11})$$

Here the sum is taken over nuclear protons. The rate of the process is readily found from the matrix element (B10):

$$\lambda_{\text{IC}} = g_s \frac{8\pi}{9} Z_X^2 \alpha^2 \left( \frac{mc}{\hbar} \right)^2 c \sqrt{\frac{E_0}{2mc^2}} |\tilde{Q}_0|^2 F(Z_X Z, E_0) \rho_1. \quad (\text{B12})$$

Here  $g_s$  is the statistical weight factor depending on the angular momenta of the initial and final states,  $m$  is the mass of the nucleus  $N$  produced as a result of the fusion reaction and  $E_0$  is its kinetic energy, which to a good accuracy coincides with the  $Q$  value of the reaction. The factor  $F(Z_X Z, E_0)$ , defined as

$$F(Z_X Z, E_0) = \frac{|\psi_f(0)|_Z^2}{|\psi_f(0)|_{Z=0}^2}, \quad (\text{B13})$$

takes into account the deviation of the wave function of the final-state nucleus  $N$  of charge  $Z$  from the plane wave due to its interaction with the electric field of the  $X$  particle. It is similar to the Fermi function employed in the theory of nuclear  $\beta$  decay. By  $\rho_1$  we denoted the quantity  $|\psi_i(0)|^2$ ; it will be discussed in more detail below.

We estimate the transition matrix elements of the charge radius operator as

$$\tilde{Q}_0 \simeq r_i r_f, \quad (\text{B14})$$

where  $r_f \equiv \langle r_c^2 \rangle_f^{1/2}$  is the rms charge radius of the final-state nucleus, and  $r_i$  is the rms charge radius of the compound nucleus in the initial state, which we express through the rms charge radii  $r_{N_1c}$  and  $r_{N_2c}$  of the fusing nuclei  $N_1$  and  $N_2$  according to Eq. (A13). Thus, we actually estimate the transition matrix element of the charge radius operator  $\tilde{Q}_0$  as the geometric mean of the charge radii of the initial and final nuclear states.

The function  $F(Z_X Z, E_0)$  can be written as

$$F(Z_X Z, E_0) = \frac{2\pi\eta}{1 - e^{-2\pi\eta}}. \quad (\text{B15})$$

The Sommerfeld parameter  $\eta$  is in this case

$$\eta = Z_X Z \alpha \sqrt{\frac{mc^2}{2E_0}}. \quad (\text{B16})$$

Note the similarity of Eq. (B15) with Eq. (B3); the difference is that Eq. (B3) describes the Coulomb repulsion

of the like-sign charged nuclei  $N_1$  and  $N_2$ , whereas Eq. (B15) accounts for the Coulomb attraction of the oppositely charged  $X$  particle and final-state nucleus  $N$  of charge  $Z$ . This attraction increases the value of the atomic wave function of  $N$  at  $r=0$  and leads to the enhancement of the reaction probability (Sommerfeld enhancement [88]).

The quantity  $\rho_1$  in Eq. (B12) is the squared modulus of the wave function of the compound nucleus in the initial state of the IC reaction, taken at zero separation between the nucleus and the  $X$  particle. We evaluate it by integrating the squared wave function of the initial atomic state ( $N_1N_2X$ ) over the distance  $\vec{r}$  between the fusing nuclei in the volume  $|\vec{r}| \leq R_{1c} + R_{2c}$  (where  $R_{1c}$  and  $R_{2c}$  are the radii of the fusing nuclei) and setting the distance  $R$  between their center of mass and the  $X$  particle to zero:

$$\rho_1 \equiv \int_{|\vec{r}| \leq r_0} |\psi_i(\vec{R} = 0, \vec{r})|^2 d^3r, \quad r_0 = R_{1c} + R_{2c}. \quad (\text{B17})$$

For our estimates we use the wave function  $\Psi_i(\vec{r}_1, \vec{r}_2)$  defined in Eq. (B6). Going from the coordinates  $\vec{r}_1$  and  $\vec{r}_2$  of  $N_1$  and  $N_2$  to their relative coordinate  $\vec{r}$  and c.m. coordinate  $\vec{R}$  and substituting into (B17), we obtain

$$\rho_1 = \frac{a_*^3}{\pi(a_1a_2)^3} \left[ 1 - e^{-\frac{2r_0}{a_*}} \left( 1 + 2\frac{r_0}{a_*} + 2\frac{r_0^2}{a_*^2} \right) \right],$$

$$a_* \equiv \left\{ \frac{m_2}{m_1 + m_2} a_1^{-1} + \frac{m_1}{m_1 + m_2} a_2^{-1} \right\}^{-1}. \quad (\text{B18})$$

#### a. Reaction ( $ddX$ ) $\rightarrow$ ${}^4\text{He} + X$ (3c)

For this reaction  $Z_1 = Z_2 = 1$ ,  $Z = 2$ , and  $Q = 23.56$  MeV. The transition matrix element of the charge radius operator, estimated according to Eqs. (B14) and (A13), is  $\tilde{Q}_0 \simeq 4.52$  fm<sup>2</sup>. For transitions from the ( $ddX$ ) state one has to take into account that the initial state of two spin-1 deuterons in the atomic  $s$  state can have total spin  $S = 2$  or  $0$  (spin 1 is excluded by Bose statistics). This gives 6 possible initial spin states. As the final-state nucleus  ${}^4\text{He}$  has zero spin and the transition operator is spin independent, the IC transition (3c) is only possible from the  $S = 0$  state of ( $ddX$ ). Therefore,  $g_s = 1/6$ . For evaluating the parameter  $\rho_1$  given in Eq. (B18) we use the values of  $a_1 = a_2 = 8.53$  fm found from the variational treatment of the ( $ddX$ ) atom with wave function (B6).

#### b. Reaction ( ${}^4\text{He}dX$ ) $\rightarrow$ ${}^6\text{Li} + X$ (6c)

In this case  $Z_1 = 2$ ,  $Z_2 = 1$ ,  $Z = 3$ , and  $Q = 0.320$  MeV. For the transition matrix element of the charge radius operator we find  $\tilde{Q}_0 \simeq 6.32$  fm<sup>2</sup>. The reaction ( ${}^4\text{He}dX$ )  $\rightarrow$   ${}^6\text{Li} + X$  is an E0 transition between nuclear states of total spin 1; therefore, the weight factor  $g_s = 1$ . For our evaluation of  $\rho_1$  we take  $a_1 = 1.81$  fm, which is the Bohr radius of the ( ${}^4\text{He}X$ ) atom, and  $a_2 \simeq 30a_1$ , as discussed in Appendix A 1 c.

The expression for the rates of IC processes can conveniently be written in the form similar to (B5):  $\lambda_{\text{IC}} = A\rho_1$ , where the reaction factor  $A$  is defined as the factor multiplying  $\rho_1$  in eq. (B12). The values of the IC reaction factor  $A$  and of the quantity  $\rho_1$  for reactions (3c) and (6c) are presented in Table II, along with the reaction factors and rates of the other discussed XCF reactions.

To assess the accuracy of our calculations of the IC reaction factors, we compared our result for the ( ${}^4\text{He}dX$ )  $\rightarrow$   ${}^6\text{Li} + X$  process with the existing calculations, which were carried out in the catalyzed BBN framework for the case of a singly charged catalyst particle  $C$  using a simple scaling law [63] and within a sophisticated coupled-channel nuclear physics approach [89]. To this end, we recalculated our result taking  $Z_X = 1$ ,  $Q = 1.3$  MeV, and the c.m. energy  $E = 10$  keV which were used in [63,89]. For the reaction factor  $A$  of the process  $d + ({}^4\text{He}C) \rightarrow {}^6\text{Li} + C$  we found  $A \equiv \lambda_{\text{IC}}/\rho_1 \simeq 9.9 \times 10^{-17}$  cm<sup>3</sup>/s. Eq. (B4) then gives for the corresponding astrophysical  $S$  factor  $S(E) = 0.19$  MeV b. This has to be compared with the results of Ref. [63] (0.3 MeV b) and Ref. [89] (0.043 MeV b). Our result lies between these two numbers, and is a factor of 1.6 smaller than the former and a factor of 4.4 larger than the latter.

## 4. Branching ratios

The rates of the subchannels of the XCF reactions in which the final state  $X$  sticks to one of the produced nuclear fragments are obtained by multiplying the total rate of the channel, given in Table II, by the corresponding sticking probability  $\omega_s$ , shown in Table III. The rate of the subchannel with a free  $X$  in the final state is then found by subtracting from the total rate of the channel the rates of all the subchannels with bound  $X$  in the final state. As an example, the rates of reactions (2b) and (2c) are obtained by multiplying the total rate of the ( $ddX$ ) fusion process with the production of  ${}^3\text{H}$  and  $p$ ,  $\lambda = 7.1 \times 10^{18}$  s<sup>-1</sup>, by  $\omega_s = 0.15$  and  $\omega_s = 1.2 \times 10^{-2}$ , respectively; the rate of reaction (2a) is then given by  $\lambda(1 - 0.15 - 1.2 \times 10^{-2})$ . It is then straightforward to find the branching ratios of all the discussed reactions; the results are presented in Table III.

- [1] J. Schechter and J. W. F. Valle, Neutrino masses in  $SU(2) \times U(1)$  theories, *Phys. Rev. D* **22**, 2227 (1980).
- [2] M. Magg and C. Wetterich, Neutrino mass problem and gauge hierarchy, *Phys. Lett.* **94B**, 61 (1980).
- [3] T. P. Cheng and L. F. Li, Neutrino masses, mixings and oscillations in  $SU(2) \times U(1)$  models of electroweak interactions, *Phys. Rev. D* **22**, 2860 (1980).
- [4] G. Lazarides, Q. Shafi, and C. Wetterich, Proton lifetime and fermion masses in an  $SO(10)$  model, *Nucl. Phys.* **B181**, 287 (1981).
- [5] R. N. Mohapatra and G. Senjanović, Neutrino masses and mixings in gauge models with spontaneous parity violation, *Phys. Rev. D* **23**, 165 (1981).
- [6] M. Lindner, M. Platscher, and F. S. Queiroz, A call for new physics: The muon anomalous magnetic moment and lepton flavor violation, *Phys. Rep.* **731**, 1 (2018).
- [7] A. Zee, A theory of lepton number violation, neutrino Majorana mass, and oscillation, *Phys. Lett.* **93B**, 389 (1980); **95B**, 461(E) (1980).
- [8] K. S. Babu, Model of 'calculable' Majorana neutrino masses, *Phys. Lett. B* **203**, 132 (1988).
- [9] J. C. Pati and A. Salam, Lepton number as the fourth color, *Phys. Rev. D* **10**, 275 (1974); **11**, 703(E) (1975).
- [10] R. N. Mohapatra and J. C. Pati, Left-right gauge symmetry and an isoconjugate model of  $CP$  violation, *Phys. Rev. D* **11**, 566 (1975).
- [11] G. Senjanović and R. N. Mohapatra, Exact left-right symmetry and spontaneous violation of parity, *Phys. Rev. D* **12**, 1502 (1975).
- [12] H. Georgi and M. Machacek, Doubly charged Higgs bosons, *Nucl. Phys.* **B262**, 463 (1985).
- [13] M. S. Chanowitz and M. Golden, Higgs boson triplets with  $M_W = M_Z \cos \theta_W$ , *Phys. Lett.* **165B**, 105 (1985).
- [14] J. F. Gunion, R. Vega, and J. Wudka, Higgs triplets in the standard model, *Phys. Rev. D* **42**, 1673 (1990).
- [15] J. F. Gunion, R. Vega, and J. Wudka, Naturalness problems for  $\rho = 1$  and other large one-loop effects for a standard model Higgs sector containing triplet fields, *Phys. Rev. D* **43**, 2322 (1991).
- [16] A. Ismail, H. E. Logan, and Y. Wu, Updated constraints on the Georgi-Machacek model from LHC Run 2, [arXiv:2003.02272](https://arxiv.org/abs/2003.02272).
- [17] J. E. Cieza Montalvo, N. V. Cortez, J. Sa Borges, and M. D. Tonasse, Searching for doubly charged Higgs bosons at the LHC in a 3-3-1 model, *Nucl. Phys.* **B756**, 1 (2006); **B796**, 422(E) (2008).
- [18] A. Alves, E. R. Barreto, A. G. Dias, C. A. de S Pires, F. S. Queiroz, and P. S. Rodrigues da Silva, Probing 3-3-1 models in diphoton Higgs boson decay, *Phys. Rev. D* **84**, 115004 (2011).
- [19] N. Arkani-Hamed, A. G. Cohen, E. Katz, A. E. Nelson, T. Gregoire, and J. G. Wacker, The minimal moose for a little Higgs, *J. High Energy Phys.* **08** (2002) 021.
- [20] A. Delgado, C. Garcia Cely, T. Han, and Z. Wang, Phenomenology of a lepton triplet, *Phys. Rev. D* **84**, 073007 (2011).
- [21] A. Alloul, M. Frank, B. Fuks, and M. Rausch de Traubenberg, Doubly-charged particles at the Large Hadron Collider, *Phys. Rev. D* **88**, 075004 (2013).
- [22] J. Alimena *et al.*, Searching for long-lived particles beyond the Standard Model at the Large Hadron Collider, *J. Phys. G* **47**, 090501 (2020).
- [23] B. S. Acharya, A. De Roeck, J. Ellis, D. K. Ghosh, R. Masełek, G. Panizzo, J. L. Pinfold, K. Sakurai, A. Shaa, and A. Wall, Prospects of searches for long-lived charged particles with MoEDAL, *Eur. Phys. J. C* **80**, 572 (2020).
- [24] M. Hirsch, R. Masełek, and K. Sakurai, Detecting long-lived multi-charged particles in neutrino mass models with MoEDAL, *Eur. Phys. J. C* **81**, 697 (2021).
- [25] R. Padhan, D. Das, M. Mitra, and A. Kumar Nayak, Probing doubly and singly charged Higgs bosons at the  $pp$  collider HE-LHC, *Phys. Rev. D* **101**, 075050 (2020).
- [26] B. Fuks, M. Nemevšek, and R. Ruiz, Doubly charged Higgs boson production at hadron colliders, *Phys. Rev. D* **101**, 075022 (2020).
- [27] P. S. B. Dev, B. Dutta, T. Ghosh, T. Han, H. Qin, and Y. Zhang, Leptonic scalars and collider signatures in a UV-complete model, *J. High Energy Phys.* **03** (2022) 068.
- [28] F. C. Frank, Hypothetical alternative energy sources for the "second meson" events, *Nature (London)* **160**, 525 (1947).
- [29] A. D. Sakharov, Passive mesons, Lebedev Inst, Report, 1948.
- [30] Ya. B. Zeldovich, Reactions induced by  $\mu$ -mesons in hydrogen, *Dokl. Akad. Nauk SSSR* **95**, 493 (1954).
- [31] L. W. Alvarez *et al.*, Catalysis of nuclear reactions by  $\mu$  mesons, *Phys. Rev.* **105**, 1127 (1957).
- [32] J. D. Jackson, Catalysis of nuclear reactions between hydrogen isotopes by  $\mu$ -mesons, *Phys. Rev.* **106**, 330 (1957).
- [33] Ya. B. Zeldovich and A. D. Sakharov, Reactions produced by  $\mu$ -mesons in hydrogen, *Zh. Eksp. Teor. Fiz.* **32**, 947 (1957) [*Sov. Phys. JETP* **5**, 775 (1957)].
- [34] Ya. B. Zeldovich, On the possible efficiency of the catalysis of nuclear reactions by mesons, *Zh. Eksp. Teor. Fiz.* **33**, 310 (1957) [*Sov. Phys. JETP* **6**, 242 (1958)].
- [35] L. N. Bogdanova and V. V. Filchenkov, Radiative and non-radiative fusion in muonic molecules, *Hyperfine Interact.*, **138**, 321 (2001).
- [36] Ya. B. Zeldovich and S. S. Gershtein, Nuclear reactions in cold hydrogen. I. Mesonic catalysis, *Usp. Fiz. Nauk* **71**, 581 (1960) [*Sov. Phys. Usp.* **3**, 593 (1961)].
- [37] S. S. Gershtein and L. I. Ponomarev, Mesomolecular processes induced by  $\mu$ - and  $\pi$ -mesons, In *Muon Physics*, edited by V. W. Hughes and C. S. Wu (Academic Press, New York, 1975), Vol. 3, pp. 141–233.
- [38] L. Bracci and G. Fiorentini, Mesic molecules and muon catalysed fusion, *Phys. Rep.* **86**, 169 (1982).
- [39] W. H. Breunlich, P. Kammel, J. S. Cohen, and M. Leon, Muon-catalyzed fusion, *Annu. Rev. Nucl. Part. Sci.* **39**, 311 (1989).
- [40] L. I. Ponomarev, Muon catalyzed fusion, *Contemp. Phys.* **31**, 219 (1990).
- [41] Y. B. Zeldovich and A. D. Sakharov, Reactions produced by  $\mu$  mesons in hydrogen, *Usp. Fiz. Nauk* **161**, 43 (1991) [*Sov. Phys. Usp.* **34**, 383 (1991)].
- [42] L. N. Bogdanova, Muon catalysis and fusion reactions at low energies, *Surv. High Energy Phys.* **6**, 177 (1992).
- [43] J. Rafelski, M. Sawicki, M. Gajda, and D. Harley, Reactions of charged massive particle in a deuterium environment, *Phys. Rev. A* **44**, 4345 (1991).

- [44] B. L. Ioffe, L. B. Okun, M. A. Shifman, and M. B. Voloshin, Heavy stable particles and cold catalysis of nuclear fusion, *Acta Phys. Pol. B* **12**, 229 (1981).
- [45] K. Hamaguchi, T. Hatsuda, and T. T. Yanagida, Stau-catalyzed nuclear fusion, [arXiv:hep-ph/0607256](https://arxiv.org/abs/hep-ph/0607256).
- [46] G. Zweig, Quark catalysis of exothermal nuclear reactions, *Science* **201**, 973 (1978).
- [47] A. Martin, Stability of three-body and four-body Coulomb systems, *Acta Phys. Hung. A* **8**, 285 (1998).
- [48] A. Krikeb, A. Martin, J.-M. Richard, and T.-T. Wu, Stability domain of systems of three arbitrary charges, *Few-Body Syst.* **29**, 237 (2000).
- [49] E. A. G. Armour, J.-M. Richard, and K. Varga, Stability of few-charge systems in quantum mechanics, *Phys. Rep.* **413**, 1 (2005).
- [50] M. Benedikt, A. Blondel, P. Janot, M. Mangano, and F. Zimmermann, Future Circular Colliders succeeding the LHC, *Nat. Phys.* **16**, 402 (2020).
- [51] R. N. Cahn and S. L. Glashow, Chemical signatures for superheavy elementary particles, *Science* **213**, 607 (1981).
- [52] A. De Rujula, S. L. Glashow, and U. Sarid, Charged dark matter, *Nucl. Phys.* **B333**, 173 (1990).
- [53] S. Hannestad, What is the lowest possible reheating temperature?, *Phys. Rev. D* **70**, 043506 (2004).
- [54] S. Burdin, M. Fairbairn, P. Mermod, D. Milstead, J. Pinfold, T. Sloan, and W. Taylor, Non-collider searches for stable massive particles, *Phys. Rep.* **582**, 1 (2015).
- [55] P. Mueller, L.-B. Wang, R. J. Holt, Z.-T. Lu, T. P. O'Connor, and J. P. Schiffer, Search for Anomalously Heavy Isotopes of Helium in the Earth's Atmosphere, *Phys. Rev. Lett.* **92**, 022501 (2004).
- [56] P. F. Smith, J. R. J. Bennett, G. J. Homer, J. D. Lewin, H. E. Walford, and W. A. Smith, A search for anomalous hydrogen in enriched D<sub>2</sub>O, using a time-of-flight spectrometer, *Nucl. Phys.* **B206**, 333 (1982).
- [57] P. Verkerk, G. Grynberg, B. Pichard, M. Spiro, S. Zylberajch, M. E. Goldberg, and P. Fayet, Search for Superheavy Hydrogen in Sea Water, *Phys. Rev. Lett.* **68**, 1116 (1992).
- [58] P. Woskov and D. Cohn, Annual Report 2009 Millimeter Wave Deep Drilling for Geothermal Energy, Natural Gas and Oil, MIT Report No. #PSFC/RR-09-11, 2009, [https://dspace.mit.edu/bitstream/handle/1721.1/93312/09rr011\\_full.pdf?sequence=1](https://dspace.mit.edu/bitstream/handle/1721.1/93312/09rr011_full.pdf?sequence=1).
- [59] J. L. Goity, W. J. Kossler, and M. Sher, Production, collection and utilization of very long-lived heavy charged leptons, *Phys. Rev. D* **48**, 5437 (1993).
- [60] D. Fargion, M. Khlopov, and C. A. Stephan, Cold dark matter by heavy double charged leptons?, *Classical Quantum Gravity* **23**, 7305 (2006).
- [61] K. M. Belotsky, M. Y. Khlopov, and K. I. Shibaev, Composite dark matter and its charged constituents, *Gravitation Cosmol.* **12**, 93 (2006).
- [62] J. R. Cudell and M. Khlopov, Dark atoms with nuclear shell: A status review, *Int. J. Mod. Phys. D* **24**, 1545007 (2015).
- [63] M. Pospelov, Particle Physics Catalysis of Thermal Big Bang Nucleosynthesis, *Phys. Rev. Lett.* **98**, 231301 (2007).
- [64] M. Pospelov and J. Pradler, Big bang nucleosynthesis as a probe of new physics, *Annu. Rev. Nucl. Part. Sci.* **60**, 539 (2010).
- [65] M. Kusakabe, G. J. Mathews, T. Kajino, and M. K. Cheoun, Review on effects of long-lived negatively charged massive particles on Big Bang Nucleosynthesis, *Int. J. Mod. Phys. E* **26**, 1741004 (2017).
- [66] ATLAS Collaboration, Search for heavy, long-lived, charged particles with large ionisation energy loss in  $pp$  collisions at  $\sqrt{s} = 13$  TeV using the ATLAS experiment and the full Run 2 dataset, [arXiv:2205.06013](https://arxiv.org/abs/2205.06013).
- [67] G. F. Giudice, M. McCullough, and D. Teresi,  $dE/dx$  from boosted long-lived particles, [arXiv:2205.04473](https://arxiv.org/abs/2205.04473).
- [68] E. Fermi and E. Teller, The capture of negative mesotrons in matter, *Phys. Rev.* **72**, 399 (1947).
- [69] A. S. Wightman, Moderation of negative mesons in hydrogen I: Moderation from high energies to capture by an H<sub>2</sub> molecule, *Phys. Rev.* **77**, 521 (1950).
- [70] J. S. Cohen, Slowing down and capture of negative muons by hydrogen: Classical-trajectory Monte Carlo calculation, *Phys. Rev. A* **27**, 167 (1983).
- [71] V. E. Markushin, Light  $\mu^-$  atoms in liquid and gaseous hydrogen and deuterium, *Zh. Eksp. Teor. Phys.* **80**, 35 (1980) [*Sov. Phys. JETP* **53**, 16 (1981)].
- [72] M. Leon and H. A. Bethe, Negative meson absorption in liquid hydrogen, *Phys. Rev.* **127**, 636 (1962).
- [73] H. Høgaasen, J.-M. Richard, and P. Sorba, Two-electron atoms, ions and molecules, *Am. J. Phys.* **78**, 86 (2010).
- [74] S. Flügge and W. Zickendrant, Berechnung von Termfolgen und Feinstrukturaufspaltung in Mesonatomen, *Z. Phys.* **143**, 1 (1955).
- [75] S. Flügge, *Practical Quantum Mechanics* (Springer-Verlag, Berlin Heidelberg, 1999), pp. 193–196.
- [76] I. Angeli and K. P. Marinova, Table of experimental nuclear ground state charge radii: An update, *At. Data Nucl. Data Tables* **99**, 69 (2013).
- [77] A. B. Migdal, Ionization of atoms in nuclear reactions, *Zh. Eksp. Teor. Fiz.* **9**, 1163 (1939).
- [78] J. M. Blatt and V. F. Weisskopf, *Theoretical Nuclear Physics* (Springer-Verlag, New York Heidelberg Berlin, 1979), p. 627.
- [79] D. D. Clayton, *Principles of Stellar Evolution and Nucleosynthesis* (University of Chicago Press, Chicago and London, 1983), Chap. 4.
- [80] O. Pisanti, G. Mangano, G. Miele, and P. Mazzella, Primordial deuterium after LUNA: Concordances and error budget, *J. Cosmol. Astropart. Phys.* **04** (2021) 020.
- [81] A. M. Mukhamedzhanov, L. D. Blokhintsev, and B. F. Irgaziev, Reexamination of the astrophysical  $S$  factor for the  $\alpha + d \rightarrow {}^6\text{Li} + \gamma$  reaction, *Phys. Rev. C* **83**, 055805 (2011).
- [82] A. Grassi, G. Mangano, L. E. Marcucci, and O. Pisanti,  $\alpha + d \rightarrow {}^6\text{Li} + \gamma$  astrophysical  $S$ -factor and its implications for Big Bang nucleosynthesis, *Phys. Rev. C* **96**, 045807 (2017).
- [83] C. Angulo *et al.*, A compilation of charged-particle induced thermonuclear reaction rates, *Nucl. Phys.* **A656**, 3 (1999).
- [84] R. S. de Souza, C. Iliadis, and A. Coc, Astrophysical  $S$ -factors, thermonuclear rates, and electron screening potential for the  ${}^3\text{He}(d,p){}^4\text{He}$  Big Bang Reaction via a hierarchical bayesian model, *Astrophys. J.* **872**, 75 (2019).



- [85] R. S. de Souza, S. R. Boston, A. Coc, and C. Iliadis, Thermonuclear fusion rates for tritium + deuterium using Bayesian methods, *Phys. Rev. C* **99**, 014619 (2019).
- [86] M. E. Rose, Theory of Internal Conversion, in: *Alpha-, Beta- and Gamma-Ray Spectroscopy*, edited by Kai Siegbahn (North-Holland, Amsterdam, 1966), Vol. 2.
- [87] A. I. Akhiezer and V. B. Berestetsky, *Quantum Electrodynamics* (Interscience, New York London Sydney, 1965), § 40.
- [88] A. Sommerfeld, Über die Beugung und Bremsung der Elektronen, *Ann. Phys. (Leipzig)* **403**, 257 (1931).
- [89] K. Hamaguchi, T. Hatsuda, M. Kamimura, Y. Kino, and T. T. Yanagida, Stau-catalyzed  ${}^6\text{Li}$  Production in Big-Bang Nucleosynthesis, *Phys. Lett. B* **650**, 268 (2007).